

1 **Decontamination industrial pharmaceutical wastewater by combining**
2 **solar photo–Fenton and biological treatment**

3
4 C. Sirtori ^{a,b,c}, A. Zapata ^a, I. Oller ^a, W. Gernjak ^{a,d}, A. Agüera ^b, S. Malato ^{a,*}

5
6 ^a *Plataforma Solar de Almería (CIEMAT), Carretera Senés, km 4, 04200 Tabernas*
7 *(Almería), Spain*

8
9 ^b *Pesticide Residue Research Group, University of Almería, 04120 Almería, Spain.*

10
11 ^c *The Capes Foundation, Ministry of Education of Brazil, PO Box 365, Brasília-DF*
12 *70359-970, Brazil.*

13
14 ^d *The University of Queensland, Advanced Water Management Centre (AWMC), Qld*
15 *4072, Australia*

16
17
18
19
20
21
22
23
24 * To whom all correspondence should be addressed

25 e-mail: sixto.malato@psa.es, Tel.: +34-950387940, fax: +34-950365015

26

27 **Abstract**

28 Characterization and treatment of a real pharmaceutical wastewater containing 775 mg
29 dissolved organic carbon per liter by a solar photo-Fenton/biotreatment was studied.
30 There were also many inorganic compounds present in the matrix. The most important
31 chemical in this wastewater was nalidixic acid (45 mg/L), an antibiotic pertaining to the
32 quinolone group. A Zahn-Wellens test demonstrated that the real bulk organic content
33 of the wastewater was biodegradable, but only after long biomass adaptation; however,
34 the nalidixic acid concentration remained constant, showing that it cannot be
35 biodegraded. An alternative is chemical oxidation (photo-Fenton process) first to
36 enhance biodegradability, followed by a biological treatment (Immobilized Biomass
37 Reactor-IBR). In this case, two studies of photo-Fenton treatment of the real wastewater
38 were performed, one with an excess of H₂O₂ (kinetic study) and another with controlled
39 H₂O₂ dosing (biodegradability and toxicity studies). In the kinetic study, nalidixic acid
40 completely disappeared after 190 minutes. In the other experiment with controlled
41 H₂O₂, nalidixic acid degradation was complete at 66 mM of H₂O₂ consumed.
42 Biodegradability and toxicity bioassays showed that photo-Fenton should be performed
43 until total degradation of nalidixic acid before coupling a biological treatment. Analysis
44 of the average oxidation state (AOS) demonstrated the formation of more oxidized
45 intermediates. With this information, the photo-Fenton treatment time (190 min) and
46 H₂O₂ dose (66 mM) necessary for adequate biodegradability of the wastewater could be
47 determined. An IBR operated in batch mode was able to reduce the remaining DOC to
48 less than 35 mg/L. Ammonium consumption and NO₃⁻ generation demonstrated that
49 nitrification was also attained in the IBR. Overall DOC degradation efficiency of the
50 combined photo-Fenton and biological treatment was over 95.97%, of which 33%
51 correspond to the solar photochemical process and 62% to the biological treatment.

52

53 *Keywords: immobilized biomass reactor, nalidixic acid, photo-Fenton, solar*
54 *photocatalysis*

55 1. Introduction

56 Industrial wastewater is often polluted by toxic or nonbiodegradable organic
57 compounds. Special attention currently focuses on pharmaceuticals (Joss et al., 2005;
58 2006). Their common consumption in human and veterinary medicine generates a
59 diverse range of residual pollutants (pharmaceuticals + metabolites) that reach the
60 aquatic environment through wastewater (Jones, 2001; Heberer., 2002). Antibiotics are
61 of particular concern, as they can induce bacterial resistance, even at low concentrations
62 (Hernández et al., 2007; Pauwels and Verstraete, 2006; Purdom et al., 1994; Schwartz et
63 al., 2003). Nalidixic acid is a synthetic antibacterial agent frequently used in the
64 treatment of urinary tract infections involving Gram-negative organisms (Othman et al.,
65 1988).

66 Alternatives to the conventional activated sludge treatment are employed for
67 nonbiodegradable or toxic industrial wastewater. Among these, chemical oxidative
68 treatments, and especially, Advanced Oxidation Processes (AOP), are well known for
69 their capacity for oxidizing and mineralizing almost any organic contaminant
70 (Cominellis et al, 2008). Nevertheless, technical applications are still scarce. As the
71 process costs may be considered the main obstacle to their commercial application,
72 several promising cost-cutting approaches have been proposed, such as integration of
73 AOPs as part of a treatment train. In the typical basic process design approach an AOP
74 pretreats nonbiodegradable or toxic wastewater, and once biodegradability has been
75 achieved, the effluent is transferred to a cheaper biological treatment. The key is to
76 minimize residence time and reagent consumption in the more expensive AOP stage by
77 applying an optimized coupling strategy (Scott and Ollis, 1997). Other proposed cost-
78 cutting measures are the use of renewable energy sources, i.e., sunlight as the irradiation
79 source for running the AOP. Photo-Fenton has been successfully demonstrated in real
80 wastewater containing high organic loads in complicated matrixes as a suitable
81 treatment for this purpose (Da Hora Machado et al., 2004; Gernjak et al., 2007; Maciel
82 et al., 2004; Moraes et al., 2004; Rodriguez de Souza et al., 2006).

83 Nevertheless, there are very few studies that combine the information of
84 chemical analysis, toxicity analysis and biodegradability analysis to study the viability
85 of the combination of photo-Fenton and biological treatment on actual industrial
86 wastewater, not only model wastewater. Some of the few available studies were
87 conducted in our group (Malato et al., 2007; Zapata et al., 2008), but these show
88 different results regarding coupling strategy for different wastewaters. Hence,

89 **Nevertheless**, there is still a major need for a scientific rationale on which an “a priori”
90 choice of the most appropriate treatment can be based **and additional case-studies like**
91 **the present one are required to enhance the common knowledge database.**

92 ~~Industrial wastewater is often polluted by toxic or nonbiodegradable organic~~
93 ~~compounds. Special attention currently focuses on pharmaceuticals [Joss et al., 2005;~~
94 ~~2006]. Their common consumption in human and veterinary medicine generates a~~
95 ~~diverse range of residual pollutants (pharmaceuticals + metabolites) that reach the~~
96 ~~aquatic environment through wastewater [Jones, 2001; Heberer., 2002]. Antibiotics are~~
97 ~~of particular concern, as they can induce bacterial resistance, even at low concentrations~~
98 ~~[Hernández et al., 2007; Pauwels and Verstraete, 2006; Purdom et al., 1994; Schwartz et~~
99 ~~al., 2003]. Nalidixic acid is a synthetic antibacterial agent frequently used in the~~
100 ~~treatment of urinary tract infections involving Gram-negative organisms [Othman et al.,~~
101 ~~1988].~~

102 The aim of this study is to provide a strategy for determining the best way of
103 combining Advanced Oxidation Processes (in this case photo-Fenton) and biological
104 treatment (immobilized biomass reactor) to achieve the mineralization and
105 detoxification of a real pharmaceutical wastewater containing nalidixic acid.

107 **2. Experimental**

108 **2.1 Chemicals**

109 The nalidixic acid standard was provided by Fluka (ref. code 70162, 25g). HPLC
110 grade methanol was supplied by Merck (Germany). A Milli-Q ultra-pure water system
111 from Millipore (Milford, MA, USA) was used throughout the study to obtain the HPLC-
112 grade water used in the analyses. Formic acid (purity, 98%) was obtained from Fluka
113 (Germany). Distilled water used in the pilot plant was supplied by the Plataforma Solar
114 de Almería (PSA) distillation plant (conductivity < 10 $\mu\text{S}/\text{cm}$, $\text{Cl}^- = 0.2\text{-}0.3 \text{ mg/L}$, NO_3^-
115 $< 0.2 \text{ mg/L}$, organic carbon $< 0.5 \text{ mg/L}$). The experiments were performed using iron
116 sulfate heptahydrate ($\text{FeSO}_4 \cdot 7\text{H}_2\text{O}$), reagent-grade hydrogen peroxide (30% w/v) and
117 sulfuric acid for pH adjustment, all purchased from Panreac. The photo-treated solutions
118 were neutralized by NaOH (reagent-grade, Panreac) for toxicity and biodegradability
119 analyses, and for discharge of the photo-treated sample into the bioreactor. Industrial
120 pharmaceutical wastewater is described in detail in the Results and Discussion section.

121

122 **2.2 Solar photochemical treatment**

123 All solar photochemical experiments were performed in a pilot-plant made up of
 124 Compound Parabolic Collectors (CPCs) designed for solar photocatalytic applications.
 125 This reactor is composed of two modules with twelve Pyrex glass tubes mounted on a
 126 fixed platform tilted 37° (local latitude). The total illuminated area is 3 m² and the
 127 volume is 40 liters, 22 l of which are irradiated volume.

128 At the beginning of all the photo-Fenton experiments, the solutions studied were
 129 directly added to the photoreactor, and a sample was taken after 15 min of
 130 homogenization (initial concentration). Then the pH was adjusted with sulfuric acid and
 131 another sample was taken after 15 min to confirm the pH. Afterwards, iron salt was also
 132 added (FeSO₄·7H₂O) and homogenized well for 15 min before a sample was taken.
 133 Finally an initial dose of hydrogen peroxide was added and samples were taken to
 134 evaluate the degradation process.

135 Photo-Fenton experiments were carried out at a pH adjusted to 2.6–2.8 (H₂SO₄,
 136 2N) and Fe²⁺ concentration of 20 mg/L. In the kinetic study, the initial hydrogen
 137 peroxide concentration was around 300 mg/L and was maintained between 200-
 138 400 mg/L during the experiments.

139 Solar ultraviolet radiation (UV) was measured by a global UV radiometer
 140 (KIPP&ZONEN, model CUV 3) mounted on a platform tilted 37° (the same as the
 141 CPCs). With Equation 1, combination of the data from several days' experiments and
 142 their comparison with other photocatalytic experiments is possible (Malato et al. 2003).

$$143 \quad t_{30W,n} = t_{30W,n-1} + \Delta t_n \frac{UV}{30} \frac{V_i}{V_T}; \quad \Delta t_n = t_n - t_{n-1} \quad (1)$$

144 Where t_n is the experimental time for each sample, UV is the average solar
 145 ultraviolet radiation measured during Δt_n , and t_{30W} is a “normalized illumination time”.
 146 In this case, time refers to a constant solar UV power of 30 W·m⁻² (typical solar UV
 147 power on a perfectly sunny day around noon). V_T is the total volume of the water loaded
 148 in the pilot plant (40 L), V_i is the total irradiated volume (22.0 L).

149

150 **2.3 Analytical determinations**

151 The nalidixic acid was analyzed by liquid chromatography (flow rate
 152 0.5 mL/min) in a HPLC–UV (Agilent Technologies, series 1100) with a C-18 column
 153 (LUNA 5 μm, 3x150mm, from Phenomenex). The isocratic method used formic acid
 154 25 mM/methanol 50/50, $\lambda=254$ nm. Ammonium and Na⁺ concentration were determined
 155 with a Dionex DX-120 ion chromatograph equipped with a Dionex Ionpac CS12A

156 4 mm x 250 mm column. Isocratic elution was done with H₂SO₄ (10 mM) at a flow rate
157 of 1.2 mL/min. Anion concentrations (NO₃⁻ and Cl⁻) were determined with a Dionex
158 DX-600 ion chromatograph using a Dionex Ionpac AS11-HC 4 mm x 250 mm column.
159 The gradient program was pre-run for 5 min with 20 mM NaOH, an 8-min injection of
160 20 mM of NaOH, and 7 min with 35 mM of NaOH, at a flow rate of 1.5 mL/min.
161 Mineralization was followed by measuring the dissolved organic carbon (DOC) by
162 direct injection of filtered samples into a Shimadzu-5050A TOC analyzer with an NDIR
163 detector and calibrated with standard solutions of potassium phthalate. Chemical
164 oxygen demand (COD) was measured with Merck® Spectroquant kits. Total iron
165 concentration was monitored by colorimetric determination with 1,10-phenanthroline,
166 following ISO 6332, using a Unicam-2 spectrophotometer. Hydrogen peroxide was
167 analyzed by a fast, simple spectrophotometric method using ammonium metavanadate,
168 which allows the H₂O₂ concentration to be determined immediately based on a red-
169 orange peroxovanadium cation formed during the reaction of H₂O₂ with metavanadate,
170 maximum absorption of which is at 450 nm. The peroxide concentrations are calculated
171 from absorption measurements by a ratio found by Nogueira et al. (2005).

172

173 **2.4 Toxicity and biodegradability assays**

174 Toxicity of the initial wastewater and selected pre-treated samples was evaluated
175 with Biofix® Lumi-10, a commercial assay. The test is based on the inhibition of the
176 luminescence emitted by the marine bacteria *Vibrio fischeri*. The reagent is a freeze-
177 dried preparation of a specially selected strain of the marine bacterium *Vibrio fischeri*
178 (formerly known as *Photobacterium phosphoreum*, NRRL number B-11177). The drop
179 in light emission was measured after contact periods of 30 minutes. Hydrogen peroxide
180 present in the samples from photo-Fenton experiments was removed prior to toxicity
181 analysis using catalase (2500 U/mg bovine liver; 100 mg/L) acquired from Fluka
182 Chemie AG (Buchs, Switzerland) after adjusting the sample pH to 7.

183 Biodegradability of the photo-Fenton pre-treated pharmaceutical wastewater at
184 different stages was evaluated by a Zahn-Wellens test (an adaptation of the EC protocol,
185 Directive 88/303/EEC). Activated sludge from the El Ejido wastewater treatment plant
186 (Almería-Spain), mineral nutrients and the test material as the sole carbon source were
187 placed together in a 0.25-L glass vessel equipped with an agitator. The test was
188 continued for 28 days at 20-25°C and under diffuse illumination (or in a dark room).
189 Degradation was monitored by DOC determination of the filtered solution, daily or at

190 other appropriate regular time intervals. The ratio of DOC eliminated after each interval
191 to initial DOC is expressed as the percentage of biodegradation. Samples analyzed are
192 considered biodegradable when the biodegradation percentage is over 70% (EPA,
193 1996).

194

195 **2.5 Biological system**

196 The selected biological reactor is an IBR (Immobilized Biomass Reactor). The
197 IBR consists of a 160-L flat-bottom tank filled with 90-95 L of polypropylene 15-mm
198 Pall Ring supports colonized by activated sludge from the conventional aerobic
199 wastewater treatment plant at El Ejido (Almería). The system is also provided with a
200 100-L conditioner tank with pH control connected to the IBR through a recirculation
201 pump. The operation flux is 500 L/h. Dissolved oxygen, pH and temperature were
202 automatically measured and registered. Total volume of both tanks was 150 L.

203 Startup and adaptation of the biological reactor began with the immobilization of
204 the sludge on the ring supports, which took two days. After this, the system was
205 maintained with controlled additions of glucose and ammonium chloride, keeping the
206 carbon/nitrogen ratio at 100/20. The next step was to adapt the sludge to high NaCl
207 content (approximately 5 g/L). During the whole adaptation process the analytical
208 controls used to evaluate the IBR state were the total suspended solid, DOC, pH and
209 Nitrogen concentration (as ammonium and nitrate).

210

211 **3. Results and discussion**

212 **3.1 Matrix characterization**

213 Firstly, the main parameters of the industrial pharmaceutical wastewater were
214 evaluated (Table 1). One relevant point was the high conductivity, associated with the
215 presence of large amounts of inorganic ions, such as chloride and sodium, found in
216 grams per litre. The sample further contained a significant concentration of suspended
217 solids, a DOC of around 775.755 mg/L and COD (chemical oxygen demand) of
218 3420 mg/L. The most important organic compound studied in the matrix was nalidixic
219 acid (Fig. 1). The concentration of this compound in the wastewater was 45 mg/L, with
220 the main DOC component being acetate.

221

222 An initial biodegradability test was performed at two different dilutions (1:2 and
223 1:8) of the original wastewater. The 1:2 dilution was selected according to the initial

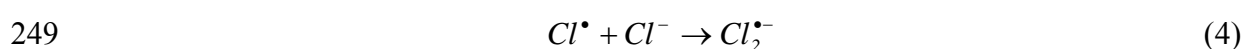
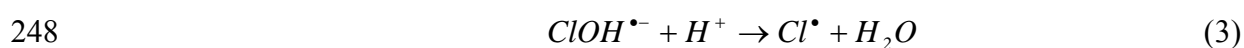
224 DOC recommended in Zahn-Wellens standard methodology. The other dilution (1:8)
 225 was studied in order to understand the behavior of sludge in contact with small
 226 concentrations of nalidixic acid. As shown in Fig 2, both samples were biodegradable.

227 However, the concentration of nalidixic acid remained constant in both cases.
 228 Adaptation also took much longer (around 15 days) for the 1:2-diluted sample, mainly
 229 due to the higher nalidixic acid concentration. This pharmaceutical may therefore be
 230 considered recalcitrant and possibly inhibitory to sludge metabolism, though not very
 231 acutely toxic. Nalidixic acid inhibition of sludge metabolism was also confirmed during
 232 photo-Fenton tests, as discussed below.

233

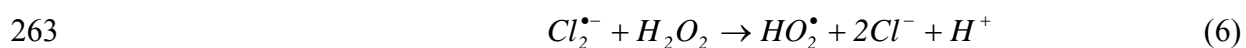
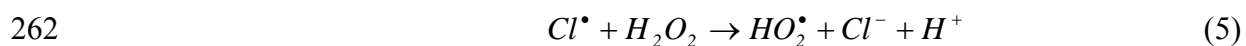
234 **3.2 Solar photo-Fenton treatment**

235 The first study was the photo-Fenton degradation of 30 mg/L of nalidixic acid
 236 standard in dematerialised saline water (5 g/L of NaCl). These conditions were selected
 237 to simulate the ionic strength of the real wastewater. The pH was kept at 2.6-2.8, the
 238 temperature 30-40 °C and Fe^{2+} concentration was 20 mg/L that is considered as
 239 optimum iron concentration for solar photoreactors selected for this study (Malato et al.,
 240 2004). The initial nalidixic acid standard mineralization rate in distilled water and with
 241 5 g/L NaCl was $0.61 \text{ mg L}^{-1} \text{ min}^{-1}$ and $0.38 \text{ mg L}^{-1} \text{ min}^{-1}$, respectively. The consumption
 242 of hydrogen peroxide at 60% mineralisation was 12 mM and 15 mM, respectively. The
 243 presence of inorganic species, like Cl^- , affects the photo-Fenton process, as Cl^- acts as a
 244 hydroxyl radical scavenger. De Laat and Le (2006) explain this by considering that less
 245 reactive species, such as chlorine atoms (Cl^\bullet) and dichloride anion radicals ($Cl_2^{\bullet-}$), are
 246 generated, by Reactions 2-4.



250 The negative effect of Cl^- on the photo-Fenton efficiency is also related to the
 251 formation of iron(III)-chlorocomplexes, concomitantly with the inhibited formation of
 252 iron(III)-hydroperoxide complexes, the reactive species in the photo-Fenton process.
 253 Nevertheless, Cl^\bullet and $Cl_2^{\bullet-}$ are strong oxidants ($E^{\circ}_{SHE}, Cl^\bullet/Cl^- = 2.41 \text{ V}$; $E^{\circ}_{SHE}, Cl_2^{\bullet-}/2Cl^-$
 254 $= 2.09 \text{ V}$) and could also oxidize organic solutes, so that the mineralization rate would
 255 not be lowered drastically. Similarly, chloride ions also make higher consumption of
 256 hydrogen peroxide necessary for the same mineralization through by Reactions 5-6. De

257 Laat and Le (2006) conclude that over 100 mM are needed to inhibit formation of
 258 iron(III)-hydroperoxide complexes and reduce the reaction rate, and that Cl^{\bullet} and $Cl_2^{\bullet-}$
 259 are reactive enough to degrade a wide range of organic compounds. Therefore, the
 260 mineralization rate of nalidixic acid dissolved in saline water (5 g/L NaCl) could be
 261 expected not to be drastically lowered.



264

265 Figure 3 shows photo-Fenton treatment of the real wastewater described in Table 1. The
 266 experimental conditions were 20 mg/L of total iron and H_2O_2 concentration was
 267 maintained between 200 and 400 mg/L. 90% of the initial DOC was removed in
 268 400 minutes of illumination time and the total H_2O_2 consumed was 180 mM. Nalidixic
 269 acid had completely disappeared at 190 minutes with 72 mM of H_2O_2 consumed. In
 270 view of these considerations, it is not recommended to mineralize 90% of DOC,
 271 because of the very long time and huge amount of hydrogen peroxide needed (around
 272 6 g/L) for such a high mineralization level. Moreover, the results shown in Figure 2
 273 show that the biodegradability of the wastewater was not bad, and therefore, nalidixic
 274 acid degradation is the main goal of treatment. So it is important to determine the
 275 behavior of biodegradability and toxicity of wastewater during the photo-Fenton
 276 treatment, mainly during nalidixic degradation and shortly afterwards to find the best
 277 treatment time with the minimum hydrogen peroxide consumption.

278

279 **3.3 Toxicity and biodegradability assays**

280 Toxicity and biodegradability of the real wastewater treated by photo-Fenton
 281 were evaluated at different stages of the process in order to determine the optimal point
 282 for coupling to the biological process.

283 To do this, it was necessary to reproduce the previous experiment maintaining
 284 all the parameters except H_2O_2 dosing the same. H_2O_2 was added so samples would be
 285 representative of the photocatalytic process. H_2O_2 was added (a small quantity, on the
 286 order of a few mM) to the photoreactor, and consumption monitored, and after the
 287 peroxide was consumed, a sample was taken for bioassay. H_2O_2 was again added, and
 288 another sample was taken after all the peroxide had been consumed. This procedure of
 289 “addition-total consumption-addition” was repeated until significant mineralization

290 (70%), ensuring that no H₂O₂ remained (which could affect the bioassays). It also
291 prevents any reaction in the dark after the sample is taken from the photoreactor, since
292 analyses are not performed until the H₂O₂ has been completely consumed. Moreover, as
293 nalidixic acid and DOC are also determined in these experiments, results can be
294 compared with the kinetic results shown in Figure 3. Another option could be to work
295 with excess H₂O₂ (as the experiment shown in Figure 3), and eliminate the remaining
296 H₂O₂ before applying the bioassay. But methods for eliminating H₂O₂ based on
297 catalase, MnO₂, etc, could change the matrix composition and/or the added chemicals
298 could change the response of the bioassays. Therefore, the data shown are directly
299 related to H₂O₂ consumption, instead of illumination time. In this experiment, 12
300 samples suitable for analyzing toxicity and biodegradability were taken (Figure 4).

301

302 Total degradation of nalidixic acid was attained at 66 mM of H₂O₂ consumed, a
303 consumption very similar to the experiment shown in Figure 3, confirming that
304 experiments performed by the “addition-total consumption-addition” procedure are
305 comparable to others in which excess H₂O₂ is added (a certain amount of H₂O₂
306 produces a specific DOC mineralization and nalidixic acid degradation). A first group
307 of samples was selected for the *Vibrio fischeri* toxicity bioassay and COD analysis (S₁,
308 S₅, S₆, S₇, S₈, S₉, S₁₁, S₁₂, S₁₃, S₁₄, S₁₅), and a second group for *Daphnia magna* toxicity
309 analysis and Zahn-Wellens test (S₆, S₉, S₁₀, S₁₂, S₁₃, S₁₄).

310 *Vibrio Fischeri* toxicity was evaluated at dilution of 1:3, 1:6 and undiluted.
311 Figure 5 shows only results with the 1:3 dilution along with DOC. All the toxicity
312 results (diluted and undiluted) were quite similar, and it can therefore be concluded that
313 photo-Fenton treatment did not decrease *Vibrio Fischeri* toxicity. *Daphnia magna*
314 bioassays demonstrated similar behavior. All microcrustaceans in all samples died in
315 24 hours. Therefore, toxicity bioassays show that photo-Fenton was unsuccessful. But
316 both bioassays have being described as very sensitive (Hernando et al., 2007) and this
317 result is not surprising for real wastewater containing hundreds of mg/L of different
318 organic compounds (for example, carboxylic acids) and their degradation intermediates.

319

320 Sometimes toxicity tests (usually a quick method) can help select the stage of an
321 AOP treatment at which the water becomes nontoxic and, presumably, biodegradable
322 (Gutiérrez et al., 2002; Hernando M.D. et al., 2005; Lapertot M. and Pulgarin C., 2006;
323 Lapertot M. et al., 2008). In other words, toxicity tests such as *Vibrio fischeri* can detect

324 toxic response in a short time (5 to 30 minutes), should be retested afterwards for
 325 biodegradability (usually a more time-consuming method). But in view of the results
 326 shown in Figure 5, no such information was found from the toxicity assays.

327 Variation in the COD during the experiment was also determined along with
 328 DOC (Figure 6). The considerable decrease in this parameter agrees with the strong
 329 oxidation of organic matter. The efficiency of the oxidative process is more clearly
 330 shown by the AOS parameter (average oxidation state), which can be calculated by
 331 Equation 7, in which DOC and COD are expressed in moles of C/L and of O₂/L,
 332 respectively, at the sampling time. AOS is between +4 for CO₂, the most oxidized state
 333 of C, and -4 for CH₄, the most reduced state of C. As observed in Figure 6, the
 334 maximum AOS of -0.3 was reached after approximately 25 mM of H₂O₂ consumed and
 335 remained around there until the end of the test. AOS usually increases with treatment
 336 time until almost reaching a plateau. These results suggest that more oxidized organic
 337 intermediates are formed at the beginning of the photocatalytic process, and after a
 338 certain time, the chemical nature of most of them no longer varies substantially (Sarria,
 339 et al., 2002), even if the photo-Fenton treatment continues. Formation of more oxidized
 340 intermediates indirectly demonstrates that the treatment can improve biodegradability.
 341 At the moment that AOS stabilizes, the chemical treatment is only mineralizing organic
 342 contaminants, but with no partial oxidation. The changes in AOS were taken into
 343 account in selecting the treatment stage at which the water might presumably be
 344 biodegradable. Zahn-Wellens tests (usually a time-consuming method) were therefore
 345 only done on samples > S₆ (H₂O₂ consumption 20 mM). Before this treatment stage the
 346 concentration of nalidixic acid and toxicity was rather high and AOS increased.

$$347 \quad \text{AOS} = \frac{4(\text{DOC} - \text{COD})}{\text{DOC}} \quad (7)$$

348 Zahn-Wellens tests (Figure 7) were performed on six **undiluted** samples at
 349 different stages during the photo-Fenton process. All samples were at least 90%
 350 biodegradable at the end of the Z-W assay. In three of them (S7, S10 and S11), in which
 351 nalidixic acid concentrations were 20.7, 8.5 and 4.6 mg/L, respectively, 70%
 352 biodegradability was attained only after 10 days of biotreatment (Samples S10 and S11
 353 after 8 days). On the other hand, samples with very low concentrations (< 1 mg/L) or
 354 without nalidixic acid (S13, S14 and S15) were biodegradable after 3 days. Results
 355 show that untreated samples need much longer adaptation periods than treated samples
 356 and that nalidixic acid (at concentration as low as 4.6 mg/L) are also detrimental in the

357 sense that they reduce biodegradation efficiency. These results demonstrated that photo-
358 Fenton should be performed until total degradation of nalidixic acid before coupling a
359 biological treatment and that AOS determination is an appropriate technique for
360 selecting those samples to be tested by Z-W assay.

361

362 **3.4 Combined solar photo-Fenton and biological system**

363 When the best photo-Fenton wastewater pretreatment for biodegradability had
364 been determined, the combined photo-Fenton/biological treatment was carried out in a
365 pilot bioreactor. Before performing the experiment in the combined system, the IBR
366 was inoculated with 150 L of concentrated activated sludge from the El Ejido
367 wastewater treatment plant (Almería, Spain). Then, recirculation was maintained
368 between the conditioner tank and the IBR in order to ensure optimum fixation of the
369 sludge on the propylene Pall Ring supports. Total suspended solids, DOC and inorganic
370 ion concentration (mainly ammonia and nitrate) were measured daily. The system was
371 maintained with controlled addition of glucose, a biodegradable pharmaceutical (CAS
372 number: 1953-04-4) less readily biodegradable than glucose, and ammonium chloride,
373 keeping the carbon/nitrogen ratio at 100/20. The next step was adapting the sludge to
374 high salinity, as the wastewater contains large quantities of NaCl (see Table 1). During
375 the whole adaptation process, NaCl concentration was increased gradually in five cycles
376 from 1 to 5 g/L.

377 Startup and adaptation of the biological reactor was done while simultaneously
378 performing several runs with the photo-Fenton reactor in order to accumulate enough
379 pre-treated wastewater to add to the bioreactor, as the photo-Fenton plant only has a
380 40 L volume and the bioreactor (IBR+conditioner tank) has 150 L. The different photo-
381 Fenton runs were accumulated in a large volume tank (neutralization tank) connected to
382 the bioreactor where the pH was adjusted roughly to 7, as automatic pH control is in the
383 bioreactor itself. In the coupled system, wastewater containing nalidixic acid (45 mg/L)
384 was pre-treated by photo-Fenton until its total elimination during 190 minutes of
385 illumination time with 20mg/L of Fe^{2+} and 66 mM of H_2O_2 consumed. The chemical
386 characterization of the photo-Fenton effluent was 530 mg/L of DOC and 6.5 g/L of
387 NaCl. It should be remarked that the same dose of H_2O_2 (66 mM) did not always
388 accomplish exactly the same mineralization, as observed in Figure 4, where less than
389 530 mg/L were attained. But the scope of the treatment was the complete (< 1 mg/L)

390 degradation of nalidixic acid. The pre-treated effluent was pumped from the
391 neutralization tank to the conditioner tank connected to the IBR.

392 The system was operated in batch mode, with a recirculation flow rate of
393 500 L/h between the conditioner tank and the IBR until the effluent was bio-mineralized
394 (final DOC 35 mg/L). The DOC and evolution of nitrogen (as NH_4^+ and NO_3^-) during
395 biological treatment are shown in Figure 8. DOC went down 495 mg/L in 4 days, a
396 result similar to the Z-W test. NH_4^+ (NH_4Cl , in a 68 mg/L concentration of N) was
397 added the first day to enable nitrifying bacteria to metabolize the organic carbon. The
398 consumption of NH_4^+ and the generation of NO_3^- demonstrated nitrification and N
399 assimilation through biomass growth as overall N content decreased.

400 Overall mineralisation efficiency of the combined photo-Fenton and biological
401 treatment in batch mode for the degradation of the real pharmaceutical wastewater was
402 over 95.97%, of which 33.27% corresponds to the solar photochemical process and
403 62.70% to the biological treatment. *Vibrio Fischeri* and *Daphnia magna* bioassays were
404 also performed on the biotreatment effluent showing below-threshold toxicity.
405 Therefore, the combined treatment was also successful from the viewpoint of
406 biotoxicity.

407

408 4. Conclusions

- 409 • It has been demonstrated that a toxic industrial wastewater containing a
410 biorecalcitrant compound (nalidixic acid) can be successfully treated by photo-
411 Fenton after long treatment with heavy consumption of hydrogen peroxide, but
412 without decreasing toxicity.
- 413 • Photo-Fenton successfully enhanced the wastewater biodegradability.
- 414 • Suitable selection of the photo-Fenton treatment time and hydrogen peroxide dose
415 necessary to reach the biodegradability threshold made it possible to degrade the
416 remaining DOC in a pilot aerobic bioreactor, and detoxify the wastewater.
- 417 • The global efficiency in the combined solar photo-Fenton+IBR system operated in
418 batch mode was 95.97% of DOC elimination (initial DOC of 775.820 mg/L), of
419 which 33.27% was accomplished by the solar photo-Fenton treatment and 62.70%
420 by the biological treatment.

421

422 Acknowledgments

423 The authors wish to thank the European Commission for financial support for
424 the INNOWATECH project under the Sixth Framework Programme, within the “Global
425 Change and Ecosystems Program” (Contract n°: 036882) and AUSTEP (Italy) for
426 providing the wastewater. Ana Zapata and Carla Sirtori thank the Spanish Ministry of
427 Education and Science and the Capes Foundation - Brazil Ministry of Education,
428 respectively, for their Ph.D. research grants.

429

430 **References**

431 Comninellis, C. Kapalka, A., Malato S., Parsons S. A., Poullos I., Mantzavinos
432 D. (2008) Advanced oxidation processes for water treatment: advances and trends for
433 R&D. *Journal of Chemical Technology and Biotechnology* 83, 769–776.

434 Da Hora Machado, A. E., Xavier, T. P., de Souza, D. R., de Miranda, J. A.,
435 Duarte, E. T. F. M., Ruggiero, R., de Oliveira, L., Sattler, C. (2004) Solar photo-Fenton
436 treatment of chipboard production wastewater. *Solar Energy* 77, 583-589.

437 De Laat, J. and Le, T.G. (2006) Effects of chloride ions on the iron(III)-
438 catalyzed decomposition of hydrogen peroxide and on the efficiency of the Fenton-like
439 oxidation process. *Applied Catalysis B: Environmental* 66, 137-146.

440 EPA-United States Environmental Protection Agency. Prevention, Pesticides
441 and Toxic Substances (7101). Fates, Transport and Transformation Test Guidelines
442 OPPTS 835.3200 Zahn-Wellens/EMPA Test. EPA 712-C-96-084 (April 1996).

443 Gernjak, W., Krutzler, T., Malato, S., Bauer, R. (2007) Photo-Fenton Treatment
444 of Olive Mill Wastewater Applying a Combined Fenton/Flocculation Pretreatment. *J.*
445 *Solar Energy Eng.* 129, 53-59.

446 Gutiérrez, M., Etxebarria, J., de las Fuentes, L. (2002) Evaluation of wastewater
447 toxicity: comparative study between microtox® and activated sludge oxygen uptake
448 inhibition. *Water Research* 36, 919-924.

449 Heberer, T. (2002) Occurrence, fate, and removal of pharmaceutical residues in
450 the aquatic environment: A review of recent research data. *Toxicology Letters* 131, 5-
451 17.

452 Hernández, F., Sancho, J. V., Ibáñez, M, Guerrero C. (2007) Antibiotic residue
453 determination in environmental waters by LC-MS. *Trends in Analytical Chemistry* 26
454 466-485.

455 Hernando, M. D., De Vettori, S., Martínez Bueno, M. J., Fernández-Alba, A.R.
456 (2007) Toxicity evaluation with *Vibrio fischeri* test of organic chemicals used in
457 aquaculture. *Chemosphere* 68, 724-730.

458 Hernando, M.D., Fernández-Alba, A.R., Tauler, R., Barceló, D. (2005) Toxicity
459 assays applied to wastewater treatment. *Talanta* 65, 358-366.

460 Jones, O.A.H., Voulvoulis, N., Lester, J.N. (2001) Human pharmaceuticals in
461 the aquatic environment a review. *Environmental Technology* 22, 1383-1394

- 462 Joss, A., Keller, E., Alder, A.C., Göbel, A., McArdell, C.S., Ternes, T.A.,
463 Siegrist, H. (2005) Removal of pharmaceuticals and fragrances in biological wastewater
464 treatment. *Water Research* 39, 3139-3152.
- 465 Joss, A., Zabczynski, S., Göbel, A., Hoffmann, B., Löffler, D., McArdell, C.S.,
466 Ternes, T.A., Thomsen, A., Siegrist, H. (2006) Biological degradation of
467 pharmaceuticals in municipal wastewater treatment: Proposing a classification scheme.
468 *Water Research* 40, 1686-1696.
- 469 Lapertot, M. and Pulgarin, C. (2006) Biodegradability assessment of several
470 priority hazardous substances: Choice, application and relevance regarding toxicity and
471 bacterial activity. *Chemosphere* 65, 682-690.
- 472 Lapertot, M., Ebrahimi, S., Oller, I., Maldonado, M.I., Gernjak, W., Malato, S.,
473 Pulgarin C. (2008) Evaluating Microtox as a tool for biodegradability assessment of
474 partially treated solutions of pesticides using Fe^{3+} and TiO_2 solar photo-assisted
475 processes. *Ecotoxicology and Environmental Safety* 69, 546–555.
- 476 Maciel, R., Sant'Anna, Jr. G.L., Dezotti, M. (2004) Phenol removal from high
477 salinity effluents using Fenton's reagents and photo-Fenton reactions. *Chemosphere* 57,
478 711-719.
- 479 Malato, S., Blanco, J., Maldonado, M.I., Oller, I., Gernjak, W., Pérez-Estrada, L.
480 (2007) Coupling solar photo-Fenton and biotreatment at industrial scale: Main results of
481 a demonstration plant. *J. Hazard. Mat.* 146(3), 440-446.
- 482 Malato, S., Blanco, J., Maldonado, M.I., Fernandez-Ibañez, P., Alarcon-Padilla
483 D., Collares-Pereira, M., Farinha-Mendes, J., Correia de Oliveira, J. (2004) Engineering
484 of solar photocatalytic collectors. *Solar Energy* 77, 513-524.
- 485 Malato, S., Blanco, J., Vidal, A., Alarcón, D., Maldonado, M. I., Cáceres, J.,
486 Gernjak, W. (2003) Applied studies in solar photocatalytic detoxification: An overview.
487 *Solar Energy* 75, 329-336.
- 488 Moraes, J. E. F., Quina, F. H., Nascimento, C. A. O., Silva, D. N., Chiavone-
489 Filho, O. (2004) Treatment of saline wastewater contaminated with hydrocarbons by the
490 photo-Fenton process. *Environmental Science and Technology* 38, 1183-1187.
- 491 Nogueira, R. F. P., Mirela, C. O., Paterlini, W. C. (2005) Simple and fast
492 spectrophotometric determination of H_2O_2 in photo-Fenton reactions using
493 metavanadate. *Talanta* 66, 86-91.
- 494 Pauwels, B. and Verstraete, W. (2006) The treatment of hospital wastewater: An
495 appraisal. *Water Health* 4, 405-416.

496 Purdom, C. E., Hardiman, P. A., Bye, V. J., Eno, N. C., Tyler, C. R., Sumpter, J.
497 P. (1994) Estrogenic effects of effluents from sewage treatment works. *Journal of*
498 *Chemical Ecology* 8 275–285;

499 Rodrigues de Souza, D., Duarte, E. T. F. M., Girardi, G. S., Velani, V., da Hora
500 Machado, A. E., Sattler, C., de Oliveira, L., de Miranda, J. A. (2006) Study of kinetic
501 parameters related to the degradation of an industrial effluent using Fenton-like
502 reactions. *Journal of Photochemistry and Photobiology A: Chemistry* 179, 269-275.

503 Othman, S., Muti, H., Shaheen, O., Awidi, A., Al-Turk, W. A. (1988) Studies on
504 the adsorption and solubility of nalidixic acid. *International Journal of Pharmaceutics*
505 41, 197-203.

506 Sarria, V., Parra, S., Adler, N., Peringer, P., Benitez, N., Pulgarin, C. (2002)
507 Recent developments in the coupling of photoassisted and aerobic biological processes
508 for the treatment of biorecalcitrant compounds. *Catalysis Today* 76, 301-315.

509 Schwartz, T., Kohnen, W., Jansen, B., Obst, U. (2003) Detection of antibiotic-
510 resistant bacteria and their resistance genes in wastewater, surface water, and drinking
511 water biofilms. *FEMS Microbiol. Ecol.* 43, 325-335.

512 Scott, J.P. and Ollis, D.F. (1997) Integration of chemical and biological
513 oxidation processes for water treatment II: recent illustrations and experiences. *Journal*
514 *of Advanced Oxidation Technology* 2, 374-381.

515 Zapata, A., Oller I., Gallay, R., Pulgarín, C., Maldonado, M.I., Malato, S. and
516 Gernjak W. (2008) Comparison of Photo-Fenton treatment and Coupled Photo-Fenton
517 and Biological Treatment for Detoxification of Pharmaceutical Industry Contaminants.
518 *J. Adv. Oxid. Techn.* 11(2), 261-269.

519

Table 1: Main parameters of industrial pharmaceutical wastewater

520

Parameter	Amount
pH	3.98
Conductivity	7 mS.cm ⁻¹
DOC	775 mg.L ⁻¹
COD	3420 mg.L ⁻¹
Acetate	1.9 g.L ⁻¹
Nalidixic acid	45 mg.L ⁻¹
TSS	0.407 g.L ⁻¹
Cl ⁻	2.8 g.L ⁻¹
PO ₄ ³⁻	0.01 g.L ⁻¹
SO ₄ ²⁻	0.16 g.L ⁻¹
Na ⁺	2 g.L ⁻¹
Ca ²⁺	0.02 g.L ⁻¹

521

522

523 **FIGURE CAPTIONS**

524

525 **Figure 1:** Chemical structure of nalidixic acid.

526

527 **Figure 2:** Zahn-Wellens biodegradability test of the pharmaceutical wastewater: 1:2 and
528 1:8 dilutions.

529

530 **Figure 3:** Mineralization of industrial pharmaceutical wastewater and H_2O_2 consumed
531 during photo-Fenton. Inset shows degradation of nalidixic acid during the same test.

532

533 **Figure 4:** Mineralization of real wastewater during the photo-Fenton process as
534 function of hydrogen peroxide dose (addition-total consumption-addition procedure). S_n
535 (from S_1 to S_{17}) are selected samples for toxicity and biodegradability studies.

536

537 **Figure 5:** Toxicity bioassay (*Vibrio fischeri*) of 1:3 diluted samples and DOC during
538 the photo-Fenton process.

539

540 **Figure 6:** AOS (see Equation 7) evolution during the photo-Fenton process.

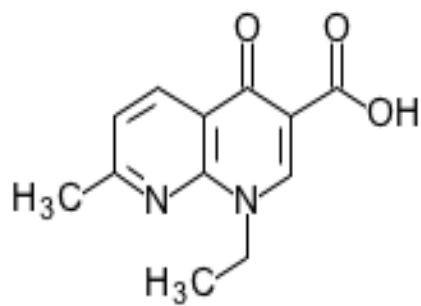
541

542 **Figure 7:** Zahn-Wellens test for selected samples during the photo-Fenton process.
543 (Initial sample is also shown)

544

545 **Figure 8:** Mineralisation of the photo-Fenton pre-treated wastewater in the IBR.

546



547

548

549

550

551

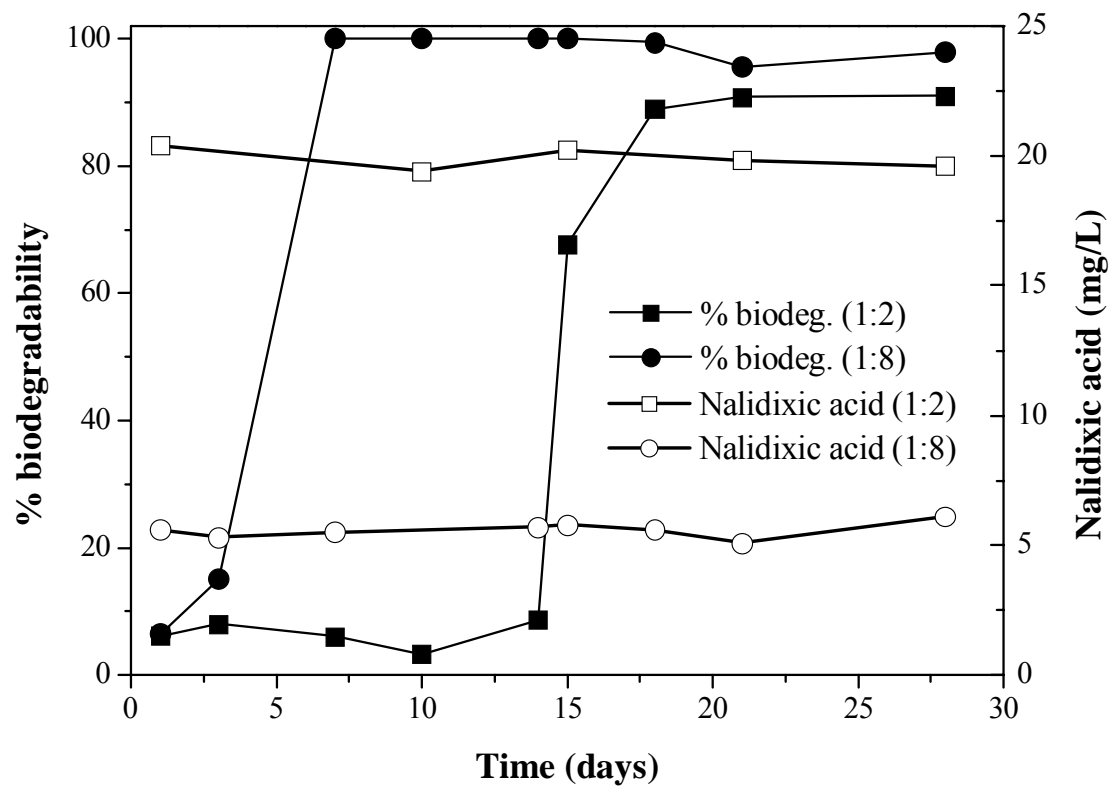
552

553

554

555

Fig. 1



556

557

558

559

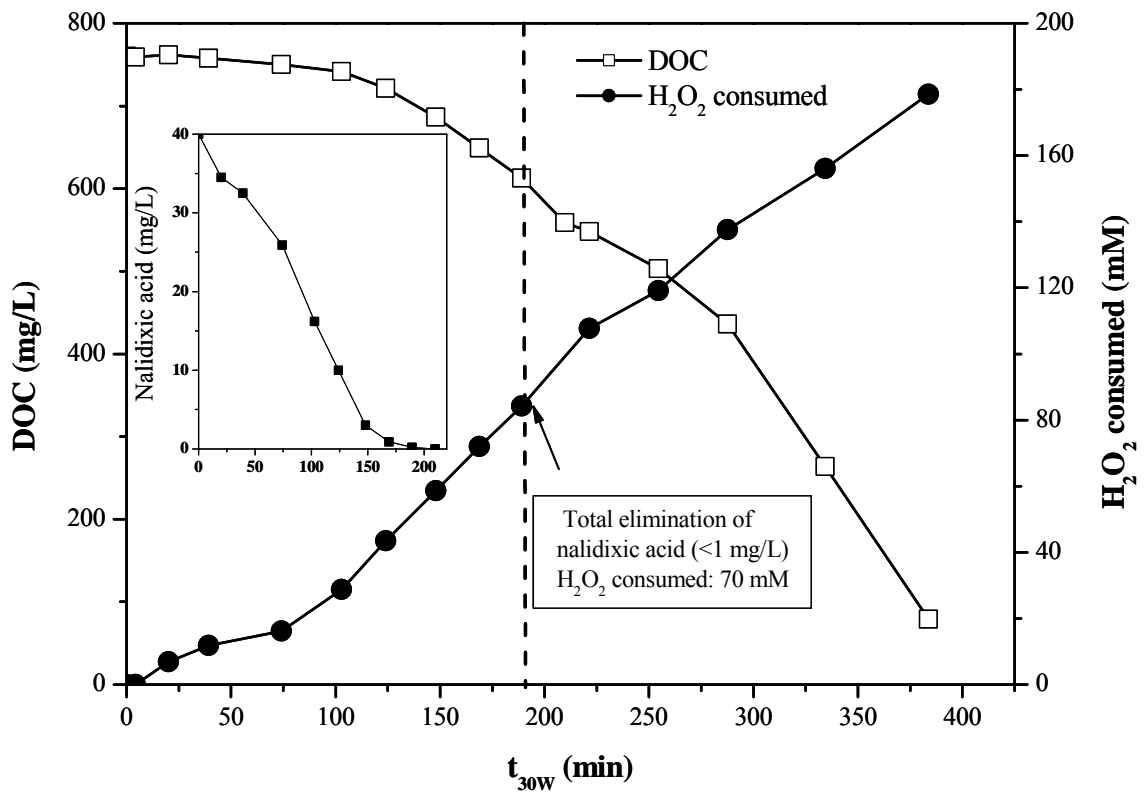
560

561

562

Fig. 2

563



564

565

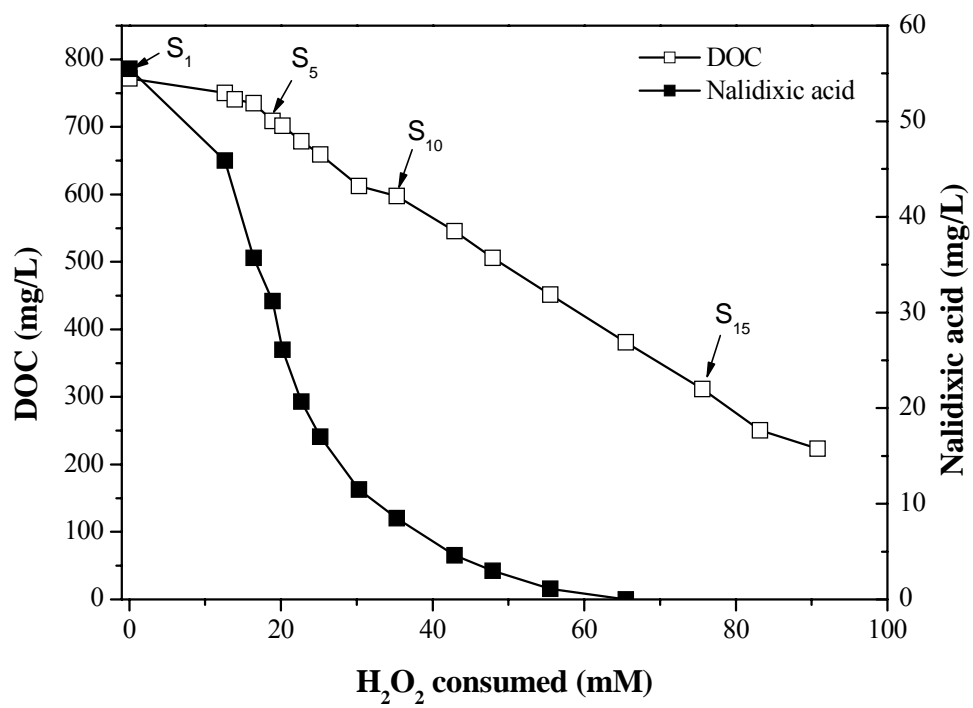
566

567

568

569

Fig. 3



570

571

572

573

574

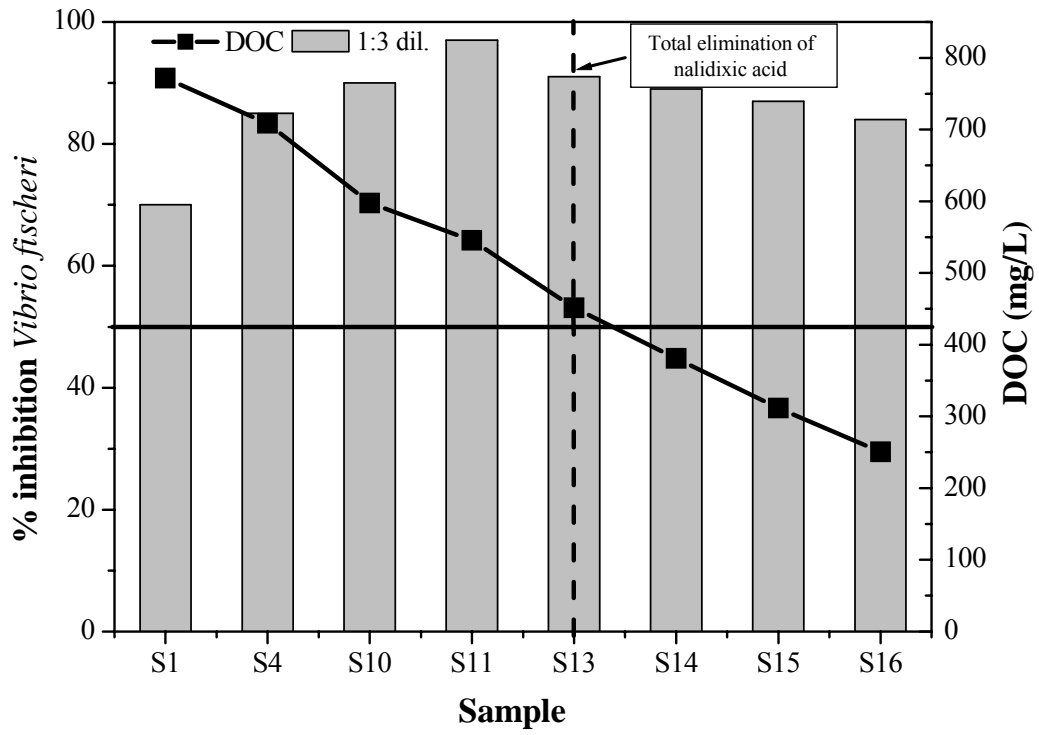
575

576

577

Fig. 4

578



579

580

581

582

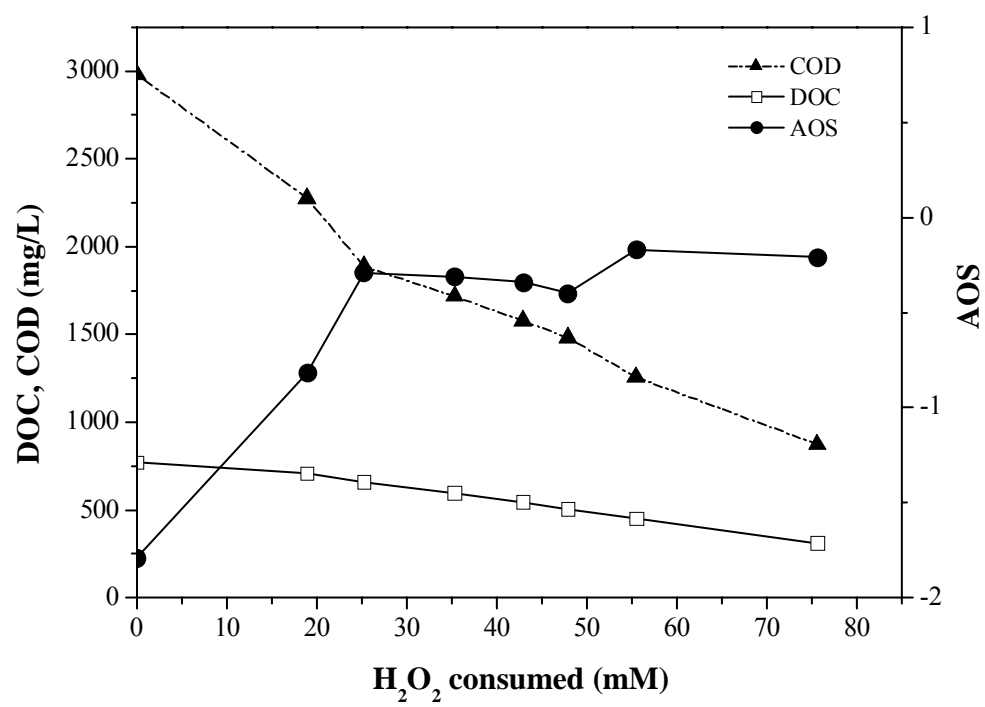
583

584

585

Fig. 5

586



587

588

589

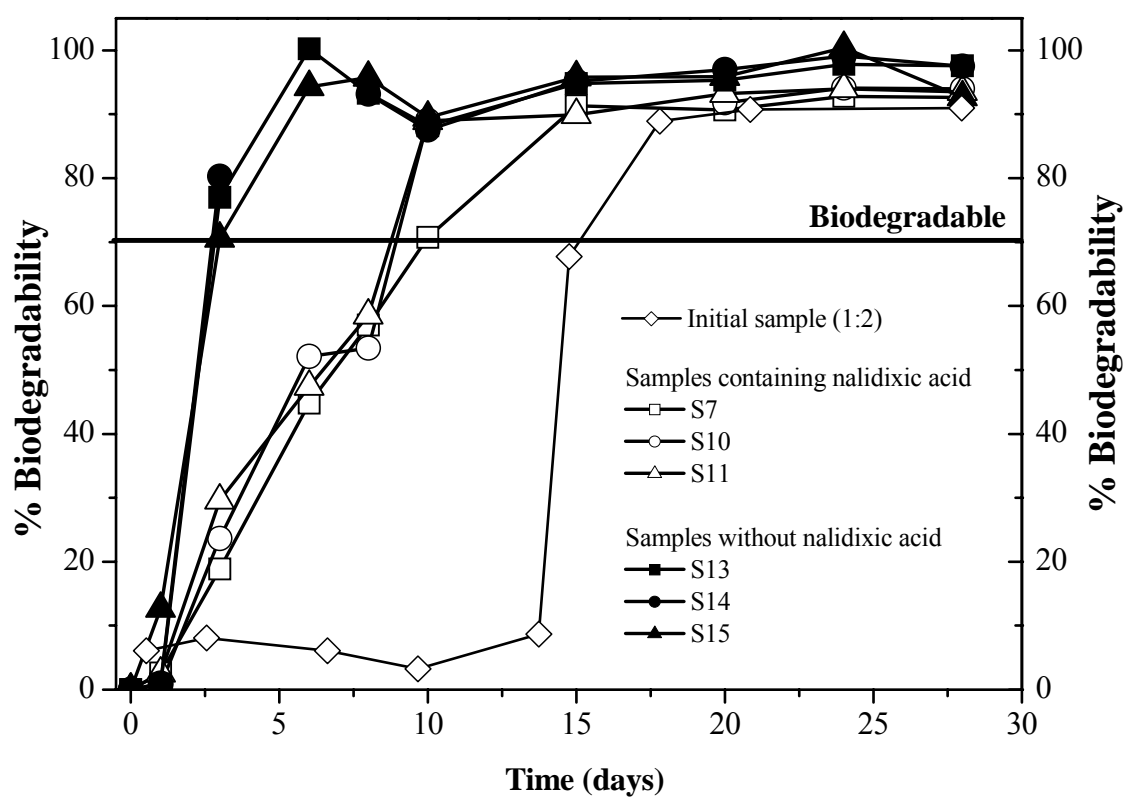
590

591

592

593

Fig. 6



594

595

596

597

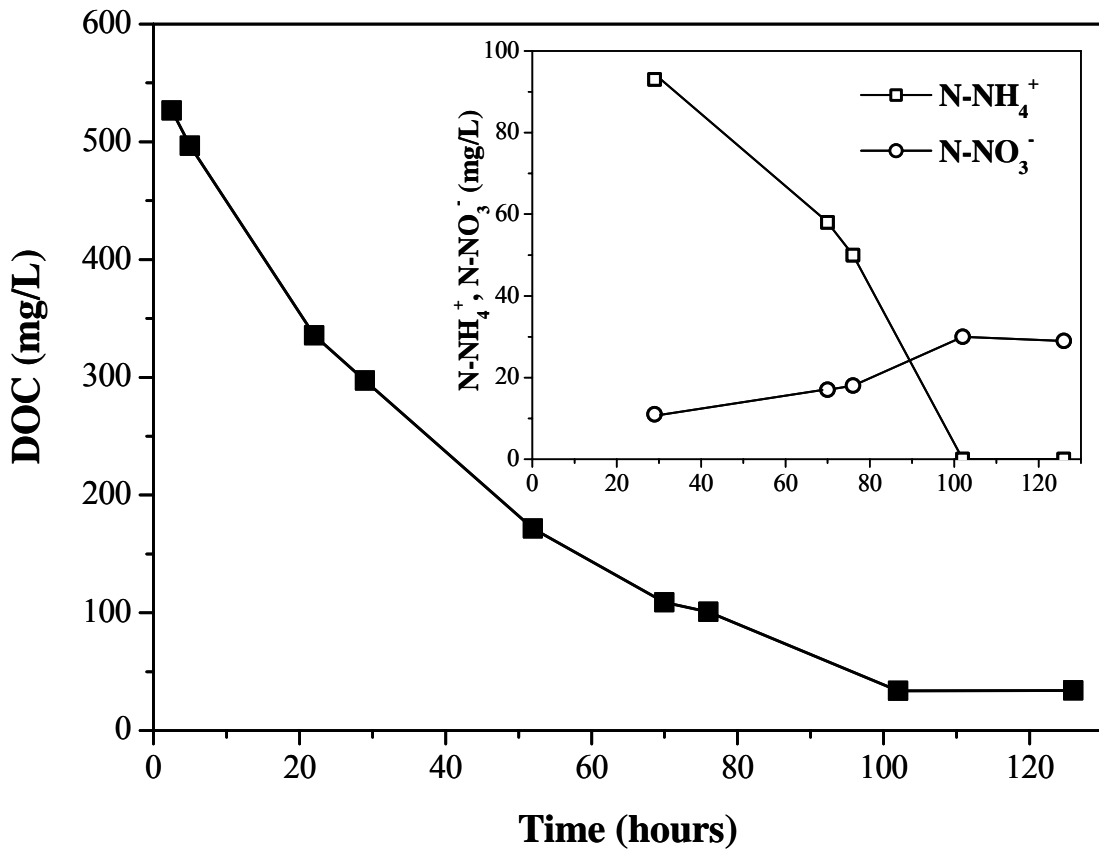
598 Fig. 7

599

600

601

602



603

604

605

606

607

608

609

Fig. 8